

# Planar–Nonplanar Conformational Equilibrium in Metal Derivatives of Octaethylporphyrin and *meso*-Nitrooctaethylporphyrin

Kelly K. Anderson,<sup>†‡</sup> J. David Hobbs,<sup>†</sup> Lian Luo,<sup>§</sup> Kimberley D. Stanley,<sup>§</sup> J. Martin E. Quirke,<sup>§</sup> and John A. Shelnutt<sup>\*,†,‡</sup>

Contribution from the Fuel Science Department 6211, Sandia National Laboratories, Albuquerque, New Mexico 87185, Department of Chemistry, University of New Mexico, Albuquerque, New Mexico 87131, and Department of Chemistry, Florida International University, Miami, Florida 33199

Received April 22, 1993. Revised Manuscript Received August 16, 1993\*

**Abstract:** The planar and nonplanar conformers of metal derivatives of 2,3,7,8,12,13,17,18-octaethylporphyrin (OEP) and 5-nitro-2,3,7,8,12,13,17,18-octaethylporphyrin (NO<sub>2</sub>-OEP) are investigated using resonance Raman spectroscopy. The structural heterogeneity is assessed by analysis of the line shapes of the structure-sensitive Raman lines. First, heterogeneity in the conformation of the macrocycle has been detected in solutions of the nickel and cobalt derivatives of OEP, that is, both planar and nonplanar conformers are found to coexist at room temperature for these metal porphyrins but not for the Cu and Zn derivatives. The latter metals expand the porphyrin core, shifting the equilibrium entirely to the planar conformer. Second, we find that substitution with a single NO<sub>2</sub> group at one of the methine-bridge carbons shifts this planar–nonplanar equilibrium substantially toward the nonplanar conformer. Thus, both crowding of the peripheral substituents and contracting of the porphyrin core (Ni(II) < Co(II) < Cu(II) < Zn(II)) displace the equilibrium toward the nonplanar conformer. Finally, the frequencies of several Raman lines correlate with structural parameters such as core size (obtained either from molecular mechanics calculations or from X-ray crystallographic studies). The calculations predict and the marker line frequencies verify that a small expansion of the core results from the steric repulsion between the nitro and the ethyl groups. Core size dependence of the intensities and frequencies of the NO<sub>2</sub> stretching vibrations suggests that the NO<sub>2</sub> stretches are coupled to nearby vibrational modes of the porphyrin macrocycle.

## Introduction

In the interest of understanding the role of nonplanar conformational distortions in modifying the biological properties of tetrapyrroles in proteins, we have undertaken the investigation of series of porphyrins in which the degree of nonplanarity varies in a systematic fashion. Nonplanarity of the tetrapyrrole has been suggested to be functionally important for a number of biological systems including the photosynthetic reaction center of *Rhodospseudomonas viridis*,<sup>1</sup> the photosynthetic antenna system of *Prosthecochloris aestuarii*,<sup>2</sup> methylreductase,<sup>3</sup> vitamin B<sub>12</sub> and B<sub>12</sub>-dependent enzymes,<sup>4</sup> and heme proteins.<sup>5</sup> In this regard, the series of nickel(II) octaalkyltetraphenylporphyrins (OATPPs) that vary in the degree of nonplanarity depending on the extent of steric crowding of the peripheral substituents was investigated.<sup>6,7</sup> For highly nonplanar octaethylphenylporphyrin (OETPP), the metal series including Ni(II), Co(II), Co(III), Cu(II), Fe(III), and Zn(II) was also examined, and the effect of the metal on the

degree of nonplanarity was determined.<sup>8</sup> In these investigations, nonplanar distortions caused by steric crowding of the peripheral substituents were meant to simulate the possible role of the protein environment in bringing about nonplanar distortions. For the metal OATPPs, the saddle-shaped nonplanar distortion is static on the time scale of optical measurements, although the saddle structure is known to invert on a much longer ( $\geq 1$  ms) time scale.

The question remains as to how well these highly substituted porphyrins reflect the properties of biologically occurring porphyrins in the protein environment. The constraints on conformational flexibility imposed by the protein matrix are certainly different from those imposed by substituent crowding in the dodecasubstituted porphyrins, and, further, the effect of the protein may be less severe. The biological porphyrins, lacking bulky meso substituents, are not greatly affected by crowding of the substituents at the periphery of the macrocycle. Nevertheless, when they contain a small metal like nickel, they exhibit nonplanar distortions in the form of interconverting planar and nonplanar conformers. A classic example is nickel(II) octaethylporphyrin (NiOEP), which in the crystalline phase is known from the X-ray

\* To whom correspondence should be addressed.

<sup>†</sup> Sandia National Laboratories.

<sup>‡</sup> University of New Mexico.

<sup>§</sup> Florida International University.

Abstract published in *Advance ACS Abstracts*, December 1, 1993.

(1) (a) Deisenhofer, J.; Michel, H. *Angew. Chem., Int. Ed. Engl.* **1989**, *28*, 829–847. (b) Deisenhofer, J.; Michel, H. *Science* **1989**, *245*, 1463–1473.

(2) Tronrud, D. E.; Schmid, M. F.; Matthews, B. W. *J. Mol. Biol.* **1986**, *188*, 443–454.

(3) (a) Eschenmoser, A. *Ann. N. Y. Acad. Sci.* **1986**, *471*, 108–129. (b) Shiemke, A. K.; Scott, R. A.; Shelnutt, J. A. *J. Am. Chem. Soc.* **1988**, *110*, 1645. (c) Shelnutt, J. A. *J. Phys. Chem.* **1989**, *93*, 6283. (d) Shiemke, A. K.; Shelnutt, J. A.; Scott, R. A. *J. Biol. Chem.* **1989**, *264*, 11236–11245. (e) Shiemke, A. K.; Kaplan, W. A.; Hamilton, C. L.; Shelnutt, J. A.; Scott, R. A. *J. Biol. Chem.* **1989**, *164*, 7276–7284. (f) Furenlid, L. R.; Renner, M. W.; Smith, K. M.; Fajer, J. *J. Am. Chem. Soc.* **1990**, *112*, 1634–1635. (g) Furenlid, L. R.; Renner, M. W.; Fajer, J. *J. Am. Chem. Soc.* **1990**, *112*, 8987–8989.

(4) Geno, M. K.; Halpern, J. *J. Am. Chem. Soc.* **1987**, *109*, 1238–1240.

(5) Takano, T. *J. Mol. Biol.* **1977**, *110*, 537.

(6) (a) Shelnutt, J. A.; Medforth, C. J.; Berber, M. D.; Barkigia, K. M.; Smith, K. M. *J. Am. Chem. Soc.* **1991**, *113*, 4077–4087. (b) The energy-minimization calculations for NiOEP predict only the planar conformer; however, for the nickel derivative we estimated in ref 6a that the nonplanar conformer is only slightly higher in energy ( $\sim 1$  kcal·mol<sup>-1</sup>). That is, the calculations predict that the planar conformer is the lowest of the two in energy but do not predict a barrier between the planar and nonplanar conformers.

(7) (a) Medforth, C. J.; Berber, M. D.; Smith, K. M.; Shelnutt, J. A. *Tetrahedron Lett.* **1990**, *31*, 3719. (b) Medforth, C. J.; Senge, M. O.; Smith, K. M.; Sparks, L. D.; Shelnutt, J. A. *J. Am. Chem. Soc.* **1992**, *114*, 9859. (c) Shelnutt, J. A.; Majumder, S. A.; Sparks, L. D.; Hobbs, J. D.; Medforth, C. J.; Senge, M. O.; Smith, K. M.; Miura, M.; Luo, L.; Quirke, J. M. E. *J. Raman Spectrosc.* **1992**, *23*, 523.

(8) Sparks, L. D.; Medforth, C. J.; Park, M.-S.; Chamberlain, J. R.; Ondrias, M. R.; Senge, M. O.; Smith, K. M.; Shelnutt, J. A. *J. Am. Chem. Soc.* **1993**, *115*, 581.

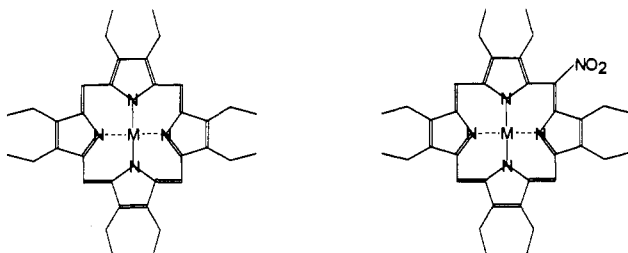


**Figure 1.** Chemical structures of metal octaethylporphyrin (left) and metal 5-nitrooctaethylporphyrin (right). (M = Ni, Co, Cu, Zn, Pd, Pt.)

structures to exist in either planar (triclinic A and B forms) or nonplanar (tetragonal form) conformations.<sup>9,10</sup> However, in noncoordinating solvents like carbon disulfide and dichloromethane, resonance Raman spectroscopy shows that these conformers coexist in equilibrium.<sup>11,12</sup> The nickel(II) derivatives of naturally occurring porphyrins like protoporphyrin and uroporphyrin also exhibit this conformational heterogeneity in solution.<sup>12</sup> Further, the conformational equilibrium between the planar and nonplanar conformers is known to be influenced when Ni protoporphyrin binds to hemoglobin in place of Fe protoporphyrin.<sup>12</sup> Thus, the planarity of biological porphyrins can be influenced both by metal size and by protein perturbations.

The present investigation addresses two important related questions concerning nonplanar distortions of porphyrins. First, how much steric interaction energy is necessary to influence the equilibrium between planar and nonplanar conformers? In particular, is the effect of addition of a single meso-nitro substituent enough to influence the equilibrium? The small perturbation caused by only one meso-nitro substituent added to octaethylporphyrin may more accurately simulate the effect that the protein environment might have on macrocycle conformation. Second, what is the effect of metal-induced core contraction upon the planar–nonplanar equilibrium? To answer these questions we have obtained resonance Raman spectra of several metal derivatives of 5-nitrooctaethylporphyrins and compared these with spectra of metal octaethylporphyrin derivatives. The chemical structures of these porphyrins are shown in Figure 1. Analysis of Raman spectra show that the nitro substituent displaces the equilibrium substantially in favor of the nonplanar conformer, and, further, the spectra indicate a strong metal core size effect on the equilibrium. With regard to biologically occurring chromophores, these results indicate that chlorophylls and hemes which contain large metals will be nonplanar in proteins only at considerable energetic expense to the protein moiety.

## Materials and Methods

**Porphyrin Synthesis.** 5-Nitro-2,3,7,8,12,13,17,18-octaethylporphyrin (NO<sub>2</sub>-OEP) was prepared by the method of Bonnett and Stephenson.<sup>13</sup> OEP (100 mg) was added to an ice-cold mixture of fuming nitric acid and glacial acetic acid (8 mL, 1:1 vol:vol). The mixture was stirred vigorously for ca. 4–5 min. The dark green solution was then poured into ice-cold water (200 mL). The mixture was extracted with methylene chloride, and the last traces of porphyrins were extracted from the aqueous layer with ether. The combined organic layers were washed twice with water and then aqueous sodium bicarbonate and finally with water again. The organic layer was evaporated and chromatographed on silica gel (200–400 mesh), using a gradient elution of toluene in hexane (from 4:1 to 2:1 vol:vol). A minor brown band of 5,10- and 5,15-dinitrooctaethylporphyrin isomers eluted in 3:1 hexane–toluene solution and was set aside. The major band, 5-nitrooctaethylporphyrin, eluted in 2:1 hexane–toluene.

(9) Brennan, T. D.; Scheidt, W. R.; Shelnut, J. A. *J. Am. Chem. Soc.* **1988**, *110*, 3919–3924.

(10) Cullen, D. L.; Meyer, E. F., Jr. *J. Am. Chem. Soc.* **1974**, *96*, 2095.

(11) Alden, R. G.; Crawford, B. A.; Doolen, R.; Ondrias, M. R.; Shelnut, J. A. *J. Am. Chem. Soc.* **1989**, *111*, 2070.

(12) Alden, R. G.; Ondrias, M. R.; Shelnut, J. A. *J. Am. Chem. Soc.* **1990**, *112*, 691–697.

(13) Bonnett, R.; Stephenson, G. F. *J. Org. Chem.* **1965**, *30*, 2791–2798.

On evaporation, the residue was recrystallized from methylene chloride–methanol (yield 60 mg, 55%).

The metal complexes of NO<sub>2</sub>-OEP were prepared according to the standard literature procedures of Buchler.<sup>14</sup> The first row transition metals incorporated into NO<sub>2</sub>-OEP were nickel(II), cobalt(II), copper(II), and zinc(II) in the order of increasing size. Zinc(II) 5-nitrooctaethylporphyrin and copper(II) 5-nitrooctaethylporphyrin were prepared by refluxing the porphyrin in methylene chloride with a solution of the appropriate metal salt in methanol. Nickel(II) 5-nitrooctaethylporphyrin and cobalt(II) 5-nitrooctaethylporphyrin were prepared according to the method of Adler *et al.*<sup>15</sup> Thus, the porphyrin was heated under reflux with the appropriate metal(II) acetate in *N,N*-dimethylformamide. Also, metals from the second (palladium(II)) and third (platinum(II)) transition rows were incorporated into NO<sub>2</sub>-OEP. Palladium(II) and platinum(II) 5-nitrooctaethylporphyrins were prepared according to the method of Eisner and Harding.<sup>16</sup> The porphyrin was refluxed with the appropriate metal(II) chloride in benzonitrile under argon. All metal complexes were recrystallized from methylene chloride–methanol (1:1 vol:vol).

The same metal derivatives of 2,3,7,8,12,13,17,18-octaethylporphyrin (OEP) were obtained from Porphyrin Products (Logan, UT) and used without further purification. All solvents were of the highest purity commercially available.

**Resonance Raman and UV–Visible Absorption Spectroscopy.** Dual-channel resonance Raman spectra of solutions of the metal OEPs and NO<sub>2</sub>-OEPs were obtained using the 413.1-nm line from a krypton ion laser (Coherent, Inc.) as the excitation source. The scattered light was collected at 90° to the direction of propagation and polarization of the exciting laser beam. Resonance Raman spectra of pairs of the metal porphyrins were obtained simultaneously using a dual-channel Raman spectrometer described elsewhere.<sup>17</sup> The spectrometer slits were adjusted to obtain a 3–4-cm<sup>-1</sup> band pass. The metal porphyrins were dissolved in CS<sub>2</sub>, and 200- $\mu$ L aliquots of two different metalloporphyrins were added to each side of a dual-compartment quartz cell. Sample concentrations were typically in a range of  $1 \times 10^{-5}$  to  $1 \times 10^{-4}$  M. Laser powers were 60 mW at the quartz cell. During the scattering experiment, the partitioned Raman cell was rotated at 50 Hz to prevent sample heating. No porphyrin decomposition was observed in the noncoordinating solvent CS<sub>2</sub> during multiple 20–30-min scans with the exception of ZnOEP.

The peak positions of the Raman lines were taken from the fast-Fourier-transform smoothed spectra. The Raman spectra were decomposed into Lorentzian line shapes using a nonlinear, least-squares curve-fitting program in which the peak frequency, peak intensity, line width, and a linear background were allowed to vary. The  $\nu_{10}$  Raman line of the Co and Ni derivatives showed anomalously broad, asymmetric line shapes; thus, two Lorentzian components were used in fitting this line. A single Lorentzian line was assumed for all other lines, even though some broadening was noted for some lines besides  $\nu_{10}$ .

UV–visible absorption spectra were obtained using an HP8452 diode array spectrophotometer (Hewlett-Packard). Absorption spectra of the porphyrins were taken in carbon disulfide by using a 1-mm-pathlength cell.

**Molecular Mechanics Calculations.** Energy-optimized structures were calculated using a force field based on the normal coordinate analyses<sup>18,19</sup> and crystal structures of NiOEP.<sup>9</sup> The force field for nickel porphyrins has been described in detail elsewhere<sup>6</sup> and has been adapted for other metals.<sup>8</sup> Core sizes are taken from both the energy-optimized structures and from X-ray crystal structures of the metal OEPs (or analogs).<sup>9,20–22</sup> The X-ray crystal structure of ZnNO<sub>2</sub>-OEP is also known from recent work.<sup>23</sup>

(14) Buchler, J. W. *Static Coordination of Metalloporphyrins. In Porphyrins and Metalloporphyrins*; Smith, K. M., Eds.; Elsevier: Amsterdam, 1975; pp 157–231. (b) Buchler, J. W. *Synthesis and Properties of Metalloporphyrins. In The Porphyrins, Vol. 1*; Dolphin, D., Ed.; Academic Press: New York, 1978; pp 389–483.

(15) Adler, A. D.; Longo, F. R.; Kampas, F.; Kim, J. *J. Inorg. Nucl. Chem.* **1970**, *32*, 2443.

(16) Eisner, U.; Harding, J. C. *Liebigs Ann. Chem.* **1974**, 1046.

(17) Shelnut, J. A. *J. Phys. Chem.* **1983**, *87*, 605.

(18) Li, X.-Y.; Czernuszewicz, R. S.; Kincaid, J. R.; Spiro, T. G. *J. Phys. Chem.* **1990**, *94*, 47.

(19) Li, X.-Y.; Czernuszewicz, R. S.; Kincaid, J. R.; Spiro, T. G. *J. Am. Chem. Soc.* **1989**, *111*, 7012–7023.

(20) Little, R. G.; Ibers, J. A. *J. Am. Chem. Soc.* **1974**, *96*, 4440.

(21) Pak, R.; Scheidt, W. R. *Acta Crystallogr.* **1991**, *C47*, 431.

(22) Cullen, D. L.; Meyer, E. F., Jr. *Acta Crystallogr.* **1976**, *B32*, 2259.

(23) Senge, M. O., personal communication.

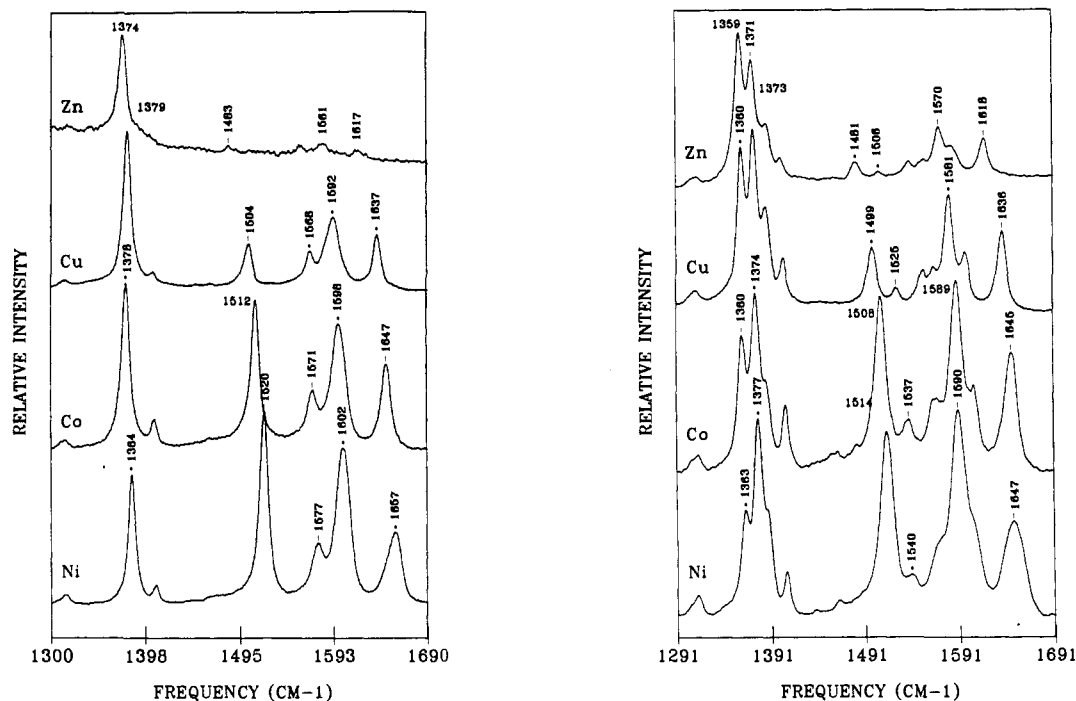


**Figure 2.** Resonance Raman spectra of metal derivatives of octaethylporphyrin (left panel) and 5-nitrooctaethylporphyrin (right panel). Spectra for (a) Ni(II), (b) Co(II), (c) Cu(II), and (d) Zn(II) porphyrin derivatives are shown in the region of the structure-sensitive Raman lines between 1300 and 1700  $\text{cm}^{-1}$ .

**Table I.** Absorption Band Maxima (nm) for Metal Derivatives of 5-Nitrooctaethylporphyrin ( $\text{NO}_2\text{-OEP}$ ) and Octaethylporphyrin (OEP) in Carbon Disulfide

| metal | metal OEP |         |          | metal $\text{NO}_2\text{-OEP}$ |         |          |
|-------|-----------|---------|----------|--------------------------------|---------|----------|
|       | $\alpha$  | $\beta$ | $\gamma$ | $\alpha$                       | $\beta$ | $\gamma$ |
| Ni    | 557       | 521     | 404      | 563                            | 527     | 405      |
| Co    | 558       | 525     | 404      | 562                            | 528     | 405      |
| Cu    | 567       | 531     | 411      | 570                            | 533     | 411      |
| Zn    | 573       | 537     | 415      | 579                            | 539     | 414      |
| Pd    | 551       | 517     | 407      | 555                            | 519     | 405      |
| Pt    | 540       | 505     | 391      | 543                            | 509     | 392      |

## Results

The wavelengths of the maxima of the absorption bands of the metal  $\text{NO}_2\text{-OEPs}$  are summarized in Table I. The wavelengths of the absorption bands of the metal OEPs are given for comparison. The usual hypsochromic metal shifts are observed for both porphyrin series.<sup>24</sup> The red bands ( $\alpha$  and  $\beta$  bands) of the metal  $\text{NO}_2\text{-OEPs}$  are red-shifted compared to their OEP counterparts.

Figure 2 shows typical resonance Raman spectra of metal derivatives of both  $\text{NO}_2\text{-OEP}$  (right panel) and, for comparison, the metal OEPs (left panel). Spectra for the nickel(II), cobalt(II), copper(II), and zinc(II) derivatives are shown in the region of the structure-sensitive Raman lines between 1300 and 1700  $\text{cm}^{-1}$ . The spectrum of ZnOEP is weak in the high-frequency region because of rapid photodecomposition during the scan. Table II gives the Raman line peak positions for the metal  $\text{NO}_2\text{-OEPs}$  and for the corresponding metal OEPs. The assignment of the strongest Raman lines in the two series of spectra is obvious when it is realized that the presence of the nitro group introduces two strong new lines into the spectra of the 5-nitro derivatives—the antisymmetric and symmetric  $\text{NO}_2$  stretching vibrations at ca. 1540 and 1360  $\text{cm}^{-1}$ , respectively. The frequencies are consistent with reported nitro stretching frequencies for aromatic nitro compounds and are tentatively assigned on this basis.<sup>25</sup> Both  $\text{NO}_2$  stretching frequencies are observed to decrease as the metal

**Table II.** Raman Line Peak<sup>a</sup> Frequencies ( $\text{cm}^{-1}$ ) for Metal Derivatives of  $\text{NO}_2\text{-OEP}$  and OEP

| metal | metal OEP |         |         |            | metal $\text{NO}_2\text{-OEP}$ |         |         |            |         |            |
|-------|-----------|---------|---------|------------|--------------------------------|---------|---------|------------|---------|------------|
|       | $\nu_4$   | $\nu_3$ | $\nu_2$ | $\nu_{10}$ | $\nu_4$                        | $\nu_3$ | $\nu_2$ | $\nu_{10}$ | $\nu_s$ | $\nu_{as}$ |
| Ni    | 1384      | 1520    | 1602    | 1657       | 1377                           | 1514    | 1590    | 1647       | 1363    | 1541       |
| Co    | 1378      | 1512    | 1598    | 1647       | 1375                           | 1508    | 1589    | 1646       | 1361    | 1538       |
| Cu    | 1379      | 1504    | 1592    | 1637       | 1373                           | 1499    | 1581    | 1636       | 1361    | 1526       |
| Zn    | 1374      | 1483    | 1581    | 1617       | 1371                           | 1481    | 1570    | 1618       | 1359    | 1506       |
| Pd    | 1382      | 1502    | 1585    | 1633       | 1376                           | 1500    | 1583    | 1633       | 1362    | 1528       |
| Pt    | 1386      | 1503    | 1594    | 1636       | 1378                           | 1502    | 1587    | 1637       | 1364    | 1535       |

<sup>a</sup> Frequencies obtained from maxima of the lines in the fast-Fourier-transform smoothed spectra.

size increases. Several weak lines of NiOEP appear to gain intensity in the spectrum of the  $\text{NO}_2\text{-OEPs}$ . Those lines include  $\nu_{20}$ ,  $\nu_{29}$ ,  $\nu_{11}$ ,  $\nu_{19}$ , and  $\nu_{38}$ , which occur in NiOEP at 1394, 1407, 1577, 1603, and 1604  $\text{cm}^{-1}$ , respectively. Increased intensity in these porphyrin modes may result from the lower molecular symmetry of  $\text{NO}_2\text{-OEPs}$ .<sup>18,19</sup>

Two other spectral trends are noteworthy. First, for both porphyrins the frequencies of the structure-sensitive lines  $\nu_4$ ,  $\nu_3$ ,  $\nu_2$ , and  $\nu_{10}$  decrease in the metal series  $\text{Ni} > \text{Co} > \text{Cu} > \text{Zn}$ , the same trend that is generally noted for the core size dependence

(25) (a) Rao, C. N. R. In *The Chemistry of the Nitro and Nitroso Groups*; Feuer, H., Ed.; John Wiley & Sons: New York, 1969; Chapter 2. (b) An electronic influence on the frequency of the nitro modes is a distinct possibility, since studies of substituted nitrobenzenes typically show a range for  $\nu_{as}$  from 1500 to 1560  $\text{cm}^{-1}$ , with the most electron-withdrawing substituents on nitrobenzene having the highest frequencies. Ortho-substitution with bulky groups in particular tends to raise the frequency of  $\nu_{as}$ . The range for ortho-substituted nitrobenzenes is similar to that for the metal derivatives of  $\text{NO}_2\text{-OEP}$ , which are from 1506  $\text{cm}^{-1}$  for Zn to 1541  $\text{cm}^{-1}$  for Ni. Thus, Ni apparently acts like an electron-withdrawing substituent and Zn like an electron-donating one. Similarly, the symmetric stretching frequency  $\nu_s$  varies from 1315 to 1360  $\text{cm}^{-1}$  for substituted nitrobenzenes but varies over only 4  $\text{cm}^{-1}$  (1363–1359) for the metal  $\text{NO}_2\text{-OEPs}$ . Again, the *o*-nitrobenzenes provide a more interesting comparison, most likely because their nitro group cannot be coplanar, as is also the case for the nitro substituent of  $\text{NO}_2\text{-OEP}$ . *o*-Nitroaniline (*e*-donating) has  $\nu_s$  at 1349  $\text{cm}^{-1}$  and  $\nu_{as}$  at 1513  $\text{cm}^{-1}$ , while *o*-(trifluoromethyl)nitrobenzene (*e*-withdrawing) has  $\nu_s$  at 1359  $\text{cm}^{-1}$  and  $\nu_{as}$  at 1539  $\text{cm}^{-1}$ . Thus,  $\nu_{as}$  differs by 26  $\text{cm}^{-1}$  between the two nitrobenzenes, while  $\nu_s$  differs by only 10  $\text{cm}^{-1}$ , that is, the behavior of the ortho-substituted anilines is much more like that of the porphyrins than the nitrobenzenes in general.

(24) Gouterman, M. In *The Porphyrins*, Vol. 3; Dolphin, D., Ed.; Academic: New York, 1978; Chapter 1.

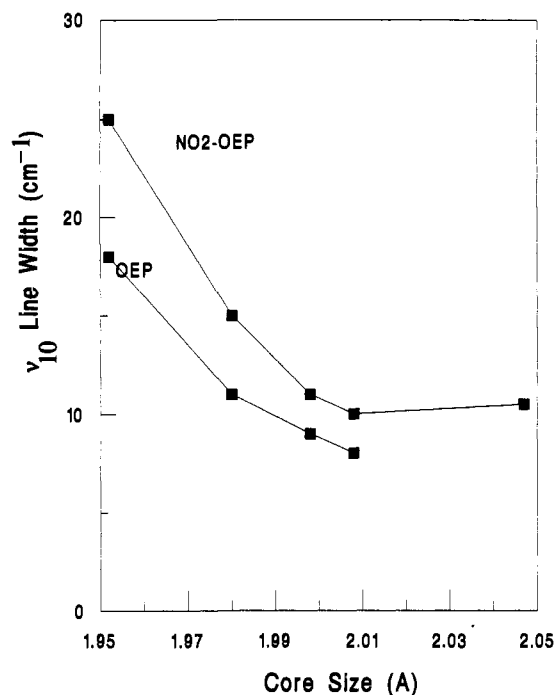


**Figure 3.** Line width of  $\nu_{10}$  in the spectra of the Ni, Co, Cu, and Pt metal octaethylporphyrin derivatives and the Ni, Co, Cu, Pt, and Zn metal 5-nitrooctaethylporphyrin derivatives plotted as a function of the metal core size (center-to-nitrogen<sub>pyrrole</sub> distance) obtained from X-ray crystal structures of the metal octaethylporphyrins.

of porphyrins with these metal ions.<sup>8</sup> Second, the Ni and Co derivatives of NO<sub>2</sub>-OEP and the Ni derivative of OEP show somewhat broader lines than the other metal derivatives. The broadening is most evident in the  $\nu_3$ ,  $\nu_2$ , and  $\nu_{10}$  lines,  $\nu_{10}$  in particular. In Figure 3, the full width at half-maximum of  $\nu_{10}$  in the spectra of the metal OEPs and the metal NO<sub>2</sub>-OEPs is plotted as a function of the metal core size (length of the projection of the metal-to-nitrogen<sub>pyrrole</sub> bond into the average plane of the porphyrin) obtained from X-ray crystal structures of the metal octaethylporphyrins or analogs. The trend is toward a minimum width of about 10 cm<sup>-1</sup> as the metal size, and hence the metal core size, increases. The platinum(II) and palladium(II) derivatives fit this trend even though they are from different rows of transition metals.

For NiOEP, the large width of the lines  $\nu_3$ ,  $\nu_2$ , and  $\nu_{10}$  has been shown to result from the coexistence of planar and nonplanar conformers in solution. Specifically, the line shape of  $\nu_{10}$  is composed of at least two component lines: one line from a planar conformer (with a frequency close to that observed in two triclinic crystalline forms in which the porphyrin ring is nearly planar) and a second line contributed by the nonplanar conformer (with a frequency intermediate between that of the planar NiOEP crystalline forms and that of the nonplanar conformer of tetragonal NiOEP crystals).

In Figure 4, the Lorentzian decomposition of the high-frequency region (1430–1700 cm<sup>-1</sup>) of the spectra of the Ni-, Co-, and CuOEPs (left panel) and NO<sub>2</sub>-OEPs (right panel) are shown. (Best fit parameters are given in Table S1 of the supplementary material.) Although at least two component lines are indicated by the broadness of lines of the Ni complexes, single lines were used in curve-fitting all lines, except for  $\nu_{10}$ , in order to lower the number of variable parameters of the least-squares fit. In addition, for all spectra the line width of  $\nu_{10}$  for the high-frequency component (planar conformer) was fixed at 10 cm<sup>-1</sup>, the average line width for the group of large metals. This procedure ensures the convergence of the least-squares fits in all cases. This 10-cm<sup>-1</sup> line width is within the error limits of other curve fits (not shown) in which the width of the planar conformer is also allowed

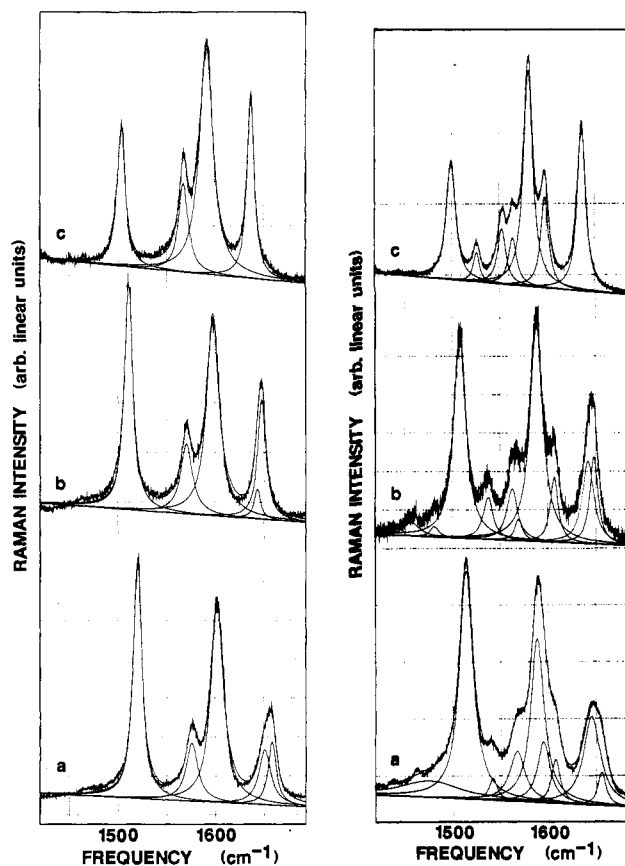


**Figure 4.** Lorentzian decomposition of the  $\nu_{10}$  resonance Raman line in the spectra of the metal derivatives of octaethylporphyrin (left panel) and 5-nitrooctaethylporphyrin (right panel): (a) nickel, (b) cobalt, (c) copper. Only one line was used for all of the modes except for  $\nu_{10}$ , reducing the number of parameters to ensure convergence. Also, the width of the planar component of  $\nu_{10}$  was fixed at 10 cm<sup>-1</sup>, further reducing the number of parameters. All other line parameters were allowed to vary in the curve fits.

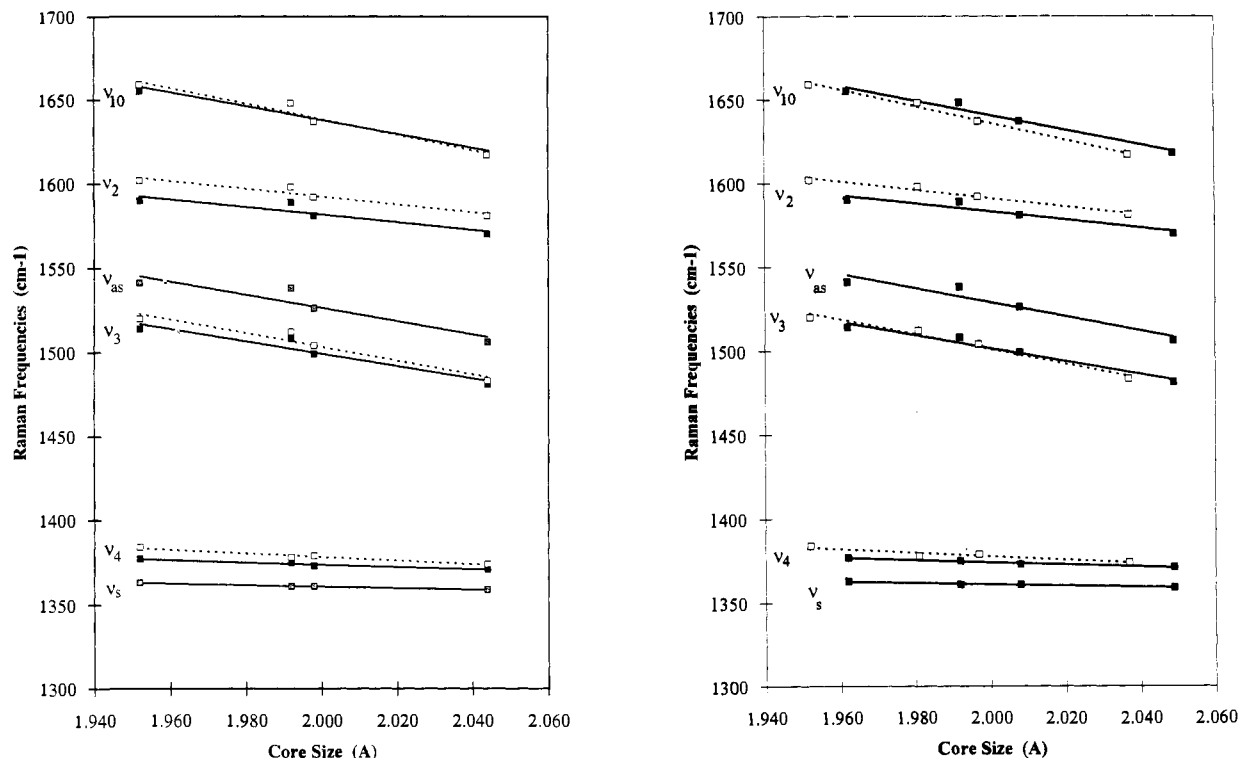
to vary. For metal porphyrins (Cu, Zn, Pt, Pd) with cores as large as or larger than copper, only one 10-cm<sup>-1</sup>-wide line was required to fit  $\nu_{10}$  well.

Figure 5 (left panel) shows the relationship between the frequencies of the structure-sensitive modes  $\nu_4$ ,  $\nu_3$ ,  $\nu_2$ , and  $\nu_{10}$  and the core size. The core size is obtained from the X-ray crystal structure of either the metallooctaethylporphyrin or the closest analog available. For the NO<sub>2</sub>-OEPs, the frequency dependence of the modes assigned to the nitro symmetric and antisymmetric stretches is also illustrated. The correlations for the metallooctaethylporphyrins are given for comparison. Figure 5 (right panel) shows the same correlations for the metal OEPs and NO<sub>2</sub>-OEPs found using calculated core sizes obtained from energy optimization. The slopes and intercepts for the linear regressions are given in Table III along with the correlation coefficients.

Comparison of the energy-optimized planar structures<sup>6a</sup> of the metal OEPs and NO<sub>2</sub>-OEPs shows that a slight expansion of the core (0.01 Å) helps to relieve the strain induced by steric repulsion between the nitro group and neighboring ethyl side chains of the porphyrin. Other systematic bond length and angle differences for the NO<sub>2</sub>-OEPs are consistent with steric strain localized at the nitro substituent.

## Discussion

**Optical Absorption Spectra.** The absorption spectra for both porphyrin series show the expected hypsochromic shifts for the metal series as described by Gouterman.<sup>24</sup> The blue (*hypso*) shift, which is largest for nickel but is also evident for cobalt and copper, results from the strong metal perturbation on the porphyrin



**Figure 5.** Correlations between Raman frequencies and core size for the metal octaethylporphyrins and metal 5-nitrooctaethylporphyrins for the structure-sensitive lines  $\nu_4$ ,  $\nu_3$ ,  $\nu_2$ , and  $\nu_{10}$ . For 5-nitrooctaethylporphyrins the symmetric ( $\nu_s$ ) and antisymmetric ( $\nu_{as}$ ) stretching modes of the nitro group are also shown. Crystallographically obtained core sizes were used in the left panel; calculated core sizes were used in the right panel. In all cases the frequencies of the planar components are plotted for  $\nu_{10}$ .

**Table III.** Slopes, Intercepts, and Correlation Coefficients<sup>a</sup> for the Raman Frequency Correlations with Core Sizes Obtained Using Metal Octaethylporphyrin or Analog Crystallographic Data and Molecular Mechanics Calculations (in parentheses)

| mode         | OEP          |                  |                       | 5-NO <sub>2</sub> -OEP |                  |                       |
|--------------|--------------|------------------|-----------------------|------------------------|------------------|-----------------------|
|              | <i>K</i>     | <i>A</i>         | <i>r</i> <sup>2</sup> | <i>K</i>               | <i>A</i>         | <i>r</i> <sup>2</sup> |
| $\nu_4$      | 107<br>(110) | 14.89<br>(14.54) | 0.960<br>(0.897)      | 66<br>(70)             | 22.75<br>(21.56) | 0.934<br>(0.973)      |
| $\nu_s$      |              |                  |                       | 43<br>(44)             | 33.50<br>(32.84) | 0.994<br>(0.960)      |
| $\nu_3$      | 410<br>(443) | 5.67<br>(5.38)   | 0.943<br>(0.977)      | 367<br>(391)           | 6.09<br>(5.84)   | 0.924<br>(0.969)      |
| $\nu_{as}$   |              |                  |                       | 392<br>(422)           | 5.89<br>(5.62)   | 0.867<br>(0.929)      |
| $\nu_2$      | 234<br>(255) | 8.82<br>(8.25)   | 0.926<br>(0.974)      | 225<br>(244)           | 9.02<br>(8.49)   | 0.840<br>(0.912)      |
| $\nu_{10}^b$ | 465<br>(503) | 5.53<br>(5.25)   | 0.955<br>(0.992)      | 412<br>(439)           | 5.98<br>(5.74)   | 0.924<br>(0.973)      |

<sup>a</sup> *K* is the slope (in  $\text{cm}^{-1}/\text{\AA}$ ); *A* is the intercept (in  $\text{\AA}$ ) according to the frequency ( $\nu$ ) versus core size ( $\delta$ ) linear relationship,  $\nu = K(A - \delta)$ ; and  $r^2$  is the correlation coefficient. <sup>b</sup> Frequencies of the planar forms are used.

$\pi \rightarrow \pi^*$  transitions that occurs for these metals but not for  $\pi$  normal metals like zinc.

The  $\alpha$  and  $\beta$  absorption bands of the metal NO<sub>2</sub>-OEPs in the red region of the visible spectrum show a bathochromic (red) shift of up to 6 nm (compared to the corresponding metal OEP). Only small differences in the Soret band are observed. The red shift of the  $\alpha$  and  $\beta$  bands is probably a result of the electron-withdrawing effect of the NO<sub>2</sub> group.<sup>26</sup> Nonplanarity can also cause a red shift in the spectra, but because the shift occurs for the Cu and Zn derivatives and these spectra are not influenced by the presence of nonplanar conformers (*vide infra*), this is not likely to be the origin of the red shifts of the metal NO<sub>2</sub>-OEPs. A red shift in the bands of the parent aromatic compound is typically observed for its nitro derivatives.<sup>25</sup>

**Resonance Raman Spectra and Structural Correlations.** The structure-sensitive Raman lines decrease in frequency for the metal derivatives in the same metal order as the spectral shifts of the absorption bands. This trend of decreasing Raman frequency with increasing metal core size for both series of porphyrins is a demonstration of the conventional core size dependence of these Raman lines for planar porphyrins.<sup>27</sup>

The correlations between porphyrin core size and Raman frequency shown in Figure 5 indicate similar dependences for the structure-sensitive modes of the metal NO<sub>2</sub>-OEPs and OEPs. The modes  $\nu_4$ ,  $\nu_3$ ,  $\nu_2$ , and  $\nu_{10}$  all have somewhat similar dependences (slopes) on core size for both porphyrin series, but the linear relationships for the NO<sub>2</sub>-OEPs are shifted to lower frequency compared to the OEPs, especially for  $\nu_2$  (Table III and Figure 5). These downshifts could be accounted for by an in-plane expansion of the core to relieve the steric repulsion between the nitro substituent and the ethyl substituents on the adjacent pyrroles. (Compare van der Waals energies in Table S2 of the supplementary material. Steric repulsion centered on the nitro substituent might also explain why the downshift is larger for  $\nu_2$  than for the other marker lines, since  $\nu_2$  consists predominantly of C <sub>$\beta$</sub> -C <sub>$\beta$</sub>  stretching motion of the pyrroles and thus likely would be most affected by steric interaction with the nitro group.) Molecular mechanics calculations predict an expansion of the core size for the nitro derivative of OEP of about 0.01  $\text{\AA}$  for all metal derivatives, as can be seen in the right panel of Figure 5. (Also, see Table S3 of the supplementary material.) This calculated core expansion is, however, not as large as estimates (up to 0.07  $\text{\AA}$ ) based on the downshift in Raman frequencies for some lines for the metal NO<sub>2</sub>-OEPs. However, the metal-nitrogen distance (2.055(8)  $\text{\AA}$ ) obtained from the crystal structure of Zn-(CH<sub>3</sub>OH)NO<sub>2</sub>-OEP<sup>23</sup> is not significantly larger than that obtained from crystal structures of the Zn(pyridine)OEP complex (2.067(6)  $\text{\AA}$ ).<sup>22</sup>

(26) Meot-Ner, M.; Adler, A. D. *J. Am. Chem. Soc.* **1975**, *97*, 5108-5111.

(27) Spaulding, L. D.; Chang, C. C.; Yu, N.-T.; Felton, R. H. *J. Am. Chem. Soc.* **1975**, *97*, 2517.

The downshifts in  $\nu_4$ ,  $\nu_3$ , and  $\nu_2$  for the NO<sub>2</sub>-OEPs are likely the result of a combination of influences including the steric effect already described, an electronic effect of the electron-withdrawing nitro substituent, and the coupling between the porphyrin modes and the nitro modes (*vide infra*). Fortunately, the frequency of  $\nu_{10}$ , the mode most sensitive to nonplanar distortion, is hardly influenced ( $\leq 1$  cm<sup>-1</sup>) by the presence of NO<sub>2</sub> substituent. Thus,  $\nu_{10}$  provides a useful measure of the nonplanar distortion of these porphyrins.

Comparison of the frequency-core size relationships for the putative nitro symmetric and antisymmetric stretching modes with the relationship for the closest porphyrin modes,  $\nu_4$  and  $\nu_3$ , respectively, shows that the nitro modes are probably coupled to the macrocycle modes. This conclusion is based on the near equality of the slopes for  $\nu_{as}$  and  $\nu_3$  and for  $\nu_s$  and  $\nu_4$  (see Table III). The similarity in the dependence on metal core size is somewhat surprising. The frequency dependence could also indicate either a distortion of the nitro group resulting from the metal-dependent contraction of the macrocycle or, more likely, an electronic interaction between the metal and the nitro group that occurs through the porphyrin orbitals.<sup>25b</sup> Finally, the intensities of the nitro modes appear to increase relative to the porphyrin modes in the metal series going from Ni to Zn. Again, similar intensity correlations have been observed in the Raman spectra of the substituted nitrobenzenes.<sup>25,28</sup>

**Porphyrin Core Size Influence on the Planar-Nonplanar Conformational Equilibrium.** Comparison of the spectra in Figure 2 clearly shows that for the Ni and Co derivatives  $\nu_{10}$  has a larger line width than for the Cu, Zn, Pd, and Pt derivatives. A similar result was previously noted for NiOEP.<sup>11</sup> Line widths for both the OEP and NO<sub>2</sub>-OEP metal series are summarized in Figure 3, where the line widths are plotted *versus* the core size of the metal OEPs. Careful examination of the line shape of  $\nu_{10}$  and other structure-sensitive lines of NiOEP indicates that the anomalous broadening of these lines is related to the coexistence of planar and nonplanar conformers in solution. Evidence includes (1) low-temperature studies, in which the components of  $\nu_{10}$  are more clearly resolved,<sup>11</sup> (2) the agreement of the frequencies of the planar and nonplanar conformers for  $\nu_{10}$ ,  $\nu_2$ , and  $\nu_3$  with those expected on the basis of Raman spectra of the planar and nonplanar crystalline forms of NiOEP,<sup>11,12</sup> and (3) changes in the line shape of  $\nu_{10}$  upon insertion of Ni protoporphyrin into apohemoglobins and other environments.<sup>12</sup>

Nonplanar distortions are promoted by small metals because the distortion allows the porphyrin core to contract around the metal, giving metal-nitrogen bond lengths that are closer to the unconstrained values. Thus, nonplanar conformers are observed for Ni and Co but not for Cu and Zn complexes whose unconstrained metal-nitrogen bond lengths are at or above the optimum porphyrin core size (2.00 Å) for a planar porphyrin.

Substituent crowding at the periphery of the porphyrin also increases the likelihood of nonplanar distortion because the nonplanar conformation relieves the steric repulsion between the substituents. From the metal NO<sub>2</sub>-OEP results, it is apparent that the introduction of only one meso-NO<sub>2</sub> group adds enough steric interaction of the peripheral substituents to shift the equilibrium in favor of the nonplanar conformer. This can be seen in Figure 4, which shows that the relative concentration of the nonplanar conformer is higher for a metal NO<sub>2</sub>-OEP than for the OEP with the corresponding metal. The relative concentrations of the conformers can be estimated from the relative areas of the component lines of  $\nu_{10}$ . (Here, we assume that the absorption spectra of the planar and nonplanar conformers are nearly identical and that the vibronic coupling matrix elements that determine the Raman intensities are nearly equal for the conformers. Both are reasonable assumptions.) For example, NiOEP is about equally distributed between the planar and

nonplanar conformers (nonplanar/planar ratio 1.63), but the Ni derivative of NO<sub>2</sub>-OEP is predominantly nonplanar (5.25). For the slightly larger Co(II) ion, almost none of the OEP is in the nonplanar conformer (0.25), whereas for the NO<sub>2</sub>-OEP, about one-half is nonplanar (1.33).

The difference in frequencies of the planar and nonplanar components of  $\nu_{10}$  gives a measure of how large the nonplanar distortion is. For example, the planar and nonplanar conformers of NiOEP differ in the frequency of  $\nu_{10}$  by 8 cm<sup>-1</sup> (1659–1651 cm<sup>-1</sup> in CS<sub>2</sub> solution). This difference should be compared to the 21-cm<sup>-1</sup> difference observed for the planar and ruffled structures in the crystalline forms of NiOEP (1662–1641 cm<sup>-1</sup>),<sup>9</sup> suggesting that the nonplanar conformer of NiOEP is less than half as distorted in CS<sub>2</sub> solution as it is in the tetragonal crystal. For CoOEP the difference is only 5 cm<sup>-1</sup>. Therefore, the larger Co ion not only reduces the concentration of the nonplanar conformer, as shown in Figure 4, but also decreases the degree of distortion in the nonplanar species.

This same trend is also observed for the Co and Ni derivatives of NO<sub>2</sub>-OEP. For Ni, the planar and nonplanar  $\nu_{10}$  frequencies are separated by 10 cm<sup>-1</sup>, a difference that is larger than for NiOEP and consistent with the predominance of the nonplanar conformer for NiNO<sub>2</sub>-OEP. Finally, the difference for the Co derivative of NO<sub>2</sub>-OEP is only 6 cm<sup>-1</sup>, consistent with there being less of the nonplanar species. Apparently, the more distorted the nonplanar conformer, the more the planar-nonplanar equilibrium will be shifted in its favor.

In this discussion we have attributed the effect of the nitro substituent on the nonplanar distortion entirely to the steric interaction at the periphery. However, an electronic effect is evident in the absorption and Raman spectra, and this electronic effect may also act to make the macrocycle more susceptible to nonplanar distortion. However, we favor the steric arguments because of our recent studies of the entire series of nickel meso-NO<sub>2</sub>-substituted OEPs, which includes the 5,10-dinitro-, 5,15-dinitro-, 5,10,15-trinitro-, and 5,10,15,20-tetranitro-substituted OEP derivatives in addition to the parent compound and the mononitro-substituted derivative investigated here.<sup>29</sup> For this series, the steric interactions increase as more nitro groups are added, resulting in increasing nonplanar distortions. Further, the molecular mechanics calculations, which include these steric interactions, predict the correct degree of nonplanar distortion to account for the decrease in frequencies of the structure-sensitive Raman lines that are observed. The calculated conformation of the tetranitrooctaethylporphyrin derivative is also in agreement with X-ray crystallographic data. Although some of the electronic effect is taken into account by the force field parameters for the nitro group, it is the steric effect that brings about the nonplanar distortion of the series of nitro-substituted porphyrins in the molecular mechanics calculations.

**Conclusions.** The most important finding of this study is that the metal clearly has an effect on the equilibrium between planar and nonplanar conformers for both OEP and NO<sub>2</sub>-OEP. Based on the ratios of the concentrations of the nonplanar and planar forms given above, we can estimate the relative energies of the two conformers using the Boltzmann distribution, and these relative energies are graphically illustrated in Figure 6. For NiOEP, the difference in the energies of the two conformers must be about  $-1.22$  kJ·mol<sup>-1</sup> ( $\exp[-\Delta E/k_B T] = \exp[-(-1.22 \text{ kJ}\cdot\text{mol}^{-1})/(2.49 \text{ kJ}\cdot\text{mol}^{-1})] = 1.63$ ), with the nonplanar form at lower energy. For CoOEP, the planar form is at lower energy and the nonplanar conformer is destabilized relative to the planar form by  $+3.45$  kJ·mol<sup>-1</sup>. For metals as large as copper, the energy of the nonplanar conformer must be greater than  $+5.73$  kJ·mol<sup>-1</sup> higher in energy than the planar conformer since nonplanar conformers are not detected (detection limit: concentration ratio

(28) Bobovich, Y. S.; Belyaevskaya, N. M. *Opt. Spektrosk.* 1965, 19, 198.

(29) Hobbs, J. D.; Majumder, S. A.; Medforth, C. J.; Luo, L.; Quirke, J. M. E.; Smith, K. M.; Shelnut, J. A. *J. Am. Chem. Soc.*, submitted for publication.

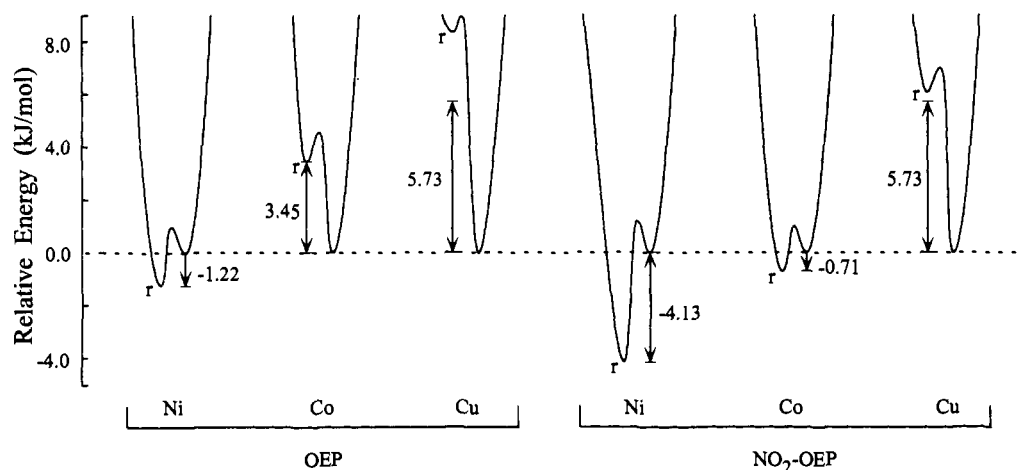


**Figure 6.** Relative free energies of the planar and nonplanar (r) conformers, calculated on the basis of the ratio of the concentrations of the two species, showing the minima for the two conformers. Only the relative energies are known for each porphyrin; the diagram for each compound is arbitrarily shifted to place the planar conformer at zero energy relative to the other porphyrins. Also, the height of the barrier between the two conformers is unknown at present. The coordinate plotted along the abscissa is the ruffling angle (0 for the planar forms).

< 0.1). Thus, the metal destabilizes the nonplanar conformer relative to the planar conformer by *more than*  $6.95 \text{ kJ}\cdot\text{mol}^{-1}$  over the Ni to Cu series of metals.

For the metal  $\text{NO}_2$ -OEP derivatives, the same trend is observed, except that the steric interactions between the nitro and ethyl substituents at the periphery tilt the equilibrium in favor of the nonplanar species by between  $2.91$  and  $4.16 \text{ kJ}\cdot\text{mol}^{-1}$  (Ni,  $-4.13 - [-1.22] = -2.91$ ; Co,  $-0.71 - [+3.45] = -4.16$ ). Therefore, for metal ions as large as or larger than copper (concentration ratio < 0.1), the ca.  $3\text{--}4 \text{ kJ}\cdot\text{mol}^{-1}$  perturbation of the nitro group is not enough to cause nonplanar distortion. To cause a shift in the equilibrium all the way to the nonplanar species (represented by  $\text{NiNO}_2$ -OEP) for a metal with a core size as large as for the copper derivative, the energy of the out-of-plane perturbation must be larger than about  $10 \text{ kJ}\cdot\text{mol}^{-1}$  ( $5.73 - [-4.13] = 9.86$ ), and the combined energy of nickel substitution for the large metal and peripheral substitution with an  $\text{NO}_2$  group is required.

Therefore, we conclude that the biologically important metals such as iron and magnesium, which have typical porphyrato core sizes (and metal–nitrogen bond lengths) in excess of about  $2.00 \text{ \AA}$ , are not likely to exhibit nonplanar structures in the absence of large ( $\geq 10 \text{ kJ}\cdot\text{mol}^{-1}$ ) external influences on the structure. Nonetheless, the protein matrix in porphyrin-containing proteins does exert considerable influence over porphyrin conformation,

particularly for the mitochondrial cytochromes *c*.<sup>12,29,30</sup> Apparently, the more severe steric crowding of substituents observed for the dodecasubstituted porphyrins is required to mimic the external forces applied by the protein environment.<sup>6–8</sup>

**Acknowledgment.** Work at Sandia National Laboratories was supported by the U.S. Department of Energy Contract DE-AC04-76DP00789. We thank Sabir Majumder for useful discussions and help in taking the initial Raman spectra.

**Supplementary Material Available:** Parameters of the Lorentzian decomposition of the spectra shown in Figure 4 (Table S1) including the areas of the components of  $\nu_{10}$  used in estimating the ratios of the concentrations of the planar and nonplanar species; other tables giving details of the molecular mechanics calculations, including the energies of optimized structures of the metal OEPs and  $\text{NO}_2$ -OEPs (Table S2) and some structural parameters obtained from the energy-minimized structures (Table S3) (2 pages). This material is contained in many libraries on microfiche, immediately follows this article in the microfilm version of the journal, and can be ordered from the ACS; see any current masthead page for ordering information.

(30) Hobbs, J. D.; Shelnut, J. A. *Biochem. J.*, submitted for publication.